FORCE BALANCES IN SYSTEMS OF CYLINDRICAL POLYELECTROLYTES

STEPHEN L. BRENNER *and* DONALD A. MCQUARRIE

From the Department of Chemistry, Indiana University, Bloomington, Indiana 47401. Dr. Brenner's present address is the Department of Chemistry, University of Kentucky, Lexington, Kentucky 40506.

ABSTRACT A detailed analysis is made of the model system of two parallel cylindrical polyelectrolytes which contain ionizable groups on their surfaces and are immersed in an ionic bathing medium. The interaction between the cylinders is examined by considering the interplay between repulsive electrostatic forces and attractive forces of electrodynamic origin. The repulsive force arises from the screened coulomb interaction between the surface charge distributions on the cylinders and has been treated by developing a solution to the linearized Poisson-Boltzmann equation. The boundary condition at the cylinder surfaces is determined as a self-consistent functional of the potential, with the input consisting of the density of ionizable groups and their dissociation constants. It is suggested that a reasonably accurate representation for the form of the attractive force can be obtained by performing a pairwise summation of the individual interatomic forces. A quantitative estimate is obtained using a Hamaker constant chosen on the basis of rigorous calculations on simpler systems. It is found that a balance exists between these repulsive and attractive forces at separations in good agreement with those observed in arrays of tobacco mosaic virus and in the A band myosin lattice in striated muscle. The behavior of the balance point as a function of the pH and ionic strength of the bathing medium closely parallels that seen experimentally.

INTRODUCTION

There are many systems of biological interest in which long cylindrical particles of macromolecular dimensions form hexagonal arrays with an interparticle center-to-center distance which may be several times the diameter of the cylinders (1–10). Detailed information is available for equilibrium gels of tobacco mosaic virus (1) and for the A band lattice of myosin in vertebrate striated muscle (2, 3). In both of these systems the interparticle distance has been demonstrated to be a function of the pH and ionic strength of the medium bathing the cylindrical particles. In 1941 Bernal and Fankuchen investigated solutions of the cylindrical tobacco-mosaic virus (length $\cong$ 3000 Å, diameter $\cong$ 170 Å), and found that in solutions containing as little as 1.8% virus, a distinct ordered phase of particles formed *spontaneously*.

X-ray analysis of the anisotropic phase indicated that the particles distribute themselves in a hexagonal assembly with a center-to-center distance varying from 170 Å (virus particles in contact) up to 1000 Å, depending on the concentration of the virus particles. Studies of the resultant ordered arrays by X-ray diffraction indicated that the distance between the particles was independent of the amount of salt solution present and dependent only on its composition. This dependence was studied as a function of the pH and ionic strength of the bathing medium. The interparticle distance was found to decrease as the pH of the bathing medium decreased until pH 3.4 where the curve exhibited a minimum with further decrease in pH resulting in an increase in the spacing of the virus particles. At constant pH the interparticle distance decreases as the ionic strength increases until a saturation value is reached, and then no further decrease in the interparticle distance occurs as the ionic strength is raised.

There is some evidence to suggest that tobacco mosaic virus *in situ* may also be arranged in ordered arrays. Wilkins et al. (4) have examined crystalline inclusions found in tobacco plants infected with tobacco mosaic virus. From their X-ray studies they have concluded that the virus particles are packed in a hexagonal array of the kind observed in vitro by Bernal and Fankuchen (1). In studies of the behavior of the A band myosin lattice in vertebrate striated muscle, Rome (2, 3) has observed behavior quite similar to that discussed above for tobacco mosaic virus particles. Although the muscle system is much more complex than the tobacco mosaic virus arrays, there is striking similarity in the lattice behavior as a function of pH and ionic strength.

Goldacre (5) has observed arrays of parallel rod-shaped bacteria in which the interparticle distance was several times the diameter of the rods. Hexagonal arrays of collagen fibers have also been observed (6, 7). Maurice (7) has observed hexagonal arrays of collagen fibers in vivo in sections of the cornea of the eye. These corneal arrays contain cylindrical collagen fibrils spaced about a diameter apart. Hexagonal patterns of microtubules are also well known, with a particularly striking example seen in the electron micrographs of the axostyle of flagellates by Grimstone (8). These microtubules are about 200 Å in diameter and are spaced about 200 Å apart. It seems likely that long-range force balances may be important in many systems containing microtubular arrays, such as cilia and flagella.

Colloid stability criteria may play an important role in the structure and function of the mitotic apparatus of the dividing cell. Inoué and Sato (9) have proposed a model for the mitotic apparatus in which the spindle fibers are made up of oriented polymers in equilibrium with dissociated monomers. They suggest that the polymer gels are weakly bound and are similar in many respects to tobacco mosaic virus gels. Oster, in his review of biocolloidal organization (10), has reaffirmed the Inoué and Sato model of the spindle and has also suggested that the motion of chromosomes during meiosis and mitosis is regulated by highly specific attractive forces, perhaps of the van der Waals variety, and a repulsion which can be regulated by the

ionic strength of the medium surrounding the chromosomes. The mechanism of cell division remains relatively poorly understood and it may be that some of the answers lie in considerations of the colloidal properties of the constituent apparatus.

It has been noted by several authors (1, 3, 6, 10–14) that the forces responsible for maintaining these lattices must be those which form the basis of the classic Derjaguin, Landau, Verwey, and Overbeek (D.L.V.O.) theory of colloid stability (15, 16). These are long range forces which involve no direct interparticle contact. Such direct contact is unlikely because of the large distances separating the particles. The D.L.V.O. theory examines the interactions of colloidal particles by considering the interplay between repulsive and attractive forces.

The repulsive force is electrostatic in origin and results from the fact that a colloidal particle usually possesses a net charge on its surface due to the dissociation of ionizable groups and/or the adsorption of ions from solution. This net charge is screened by the increase in concentration of counterions in the vicinity of the charged particle. The tendency of these counterions to approach the charged surface is counteracted by their random thermal motion, producing a diffuse ionic double layer around the particle. When two colloidal particles of like charge approach each other, their double layers interpenetrate and a repulsive force results due to the interaction of the unscreened surface charge.

The modern theory of attractive van der Waals forces was developed over 16 years ago with the major impetus given in the classic work of Lifshitz and co-workers (17, 18) in the mid-1950's. The basic idea behind the Lifshitz theory is that an attractive force is present between neutral macroscopic bodies (macroscopic here means large compared with atomic dimensions) because of the fluctuating electromagnetic field which is always present in the interior of any absorbing medium and also extends beyond its boundaries. This field is due to fluctuations in the position and motion of the charges in the body which produce spontaneous electric and magnetic moments. In essence, Lifshitz regards this entire set of local spontaneous electric field fluctuations as an electromagnetic field which extends over the whole system. This time-varying field can be frequency analyzed; the strength of the field at a particular frequency is directly dependent upon the response of the material to an applied field of that frequency, i.e., its frequency-dependent dielectric constant. The correlation of the fields due to two macroscopic bodies is of such a nature as to lower the energy and thus produce an attractive force. The beauty of the Lifshitz formulation is that it requires only a knowledge of the macroscopic absorption properties of the constituent materials in order to calculate the attractive dispersion force.

Because it is formulated through a continuum picture, the theory includes all many-body forces, retains contributions from all interaction frequencies, and deals correctly with the effects of substances between the interacting bodies (e.g., water between hydrocarbon regions). Before the development of the Lifshitz theory, estimates of the dispersion energy between colloidal particles had been severely

limited by several *ad hoc* assumptions which include simple pairwise additivity of the individual atomic interactions between the interacting bodies, the assumption that contributions centered around a single dominant frequency in the ultraviolet are important, and the difficulty of dealing with intermediate substances. The incorporation of the Lifshitz formulation into the D.L.V.O. theory has been begun only recently by Ninham and Parsegian (19–23), and their studies have indicated that the application of the classic D.L.V.O. techniques for computing the van der Waals force can, at best, give only a qualitative picture of the attractive force.

The purpose of this study is to develop techniques for analyzing the forces between cylindrical macromolecules in solution, to investigate whether a balance between the repulsive and attractive forces can be achieved at reasonable separations between the cylinders, and to determine how that balance is altered by modifying the environment of the cylinders. Elliott (24) has presented such an analysis in an effort to explain Rome's data on the A band lattice of myosin (2, 3) but his efforts fall short in several respects as will be discussed in more detail later. Miller and Woodhead-Galloway (14) have also presented an analysis of these forces. For the electrostatic and van der Waals forces they adopt asymptotic functional forms valid only on very close approach of the cylinders. They then use these equations at large separations and so the results of their analysis cannot be considered at all quantitative. Nevertheless, the basic idea of a force balance between two cylinders is contained in their paper, and their study provided the initial motivation for this work. Shear (12, 13) has proposed a model for muscular contraction based upon long-range electrostatic forces, but he has neglected van der Waals forces and has treated the electrostatics in a severely approximate way. In this work, we develop the theory of the electrostatic interaction between cylindrical polyelectrolytes using an analogue of the technique proposed by Levine (25, 26) for spherical metallic particles. The model system consists of two parallel cylindrical polyelectrolytes containing ionizable groups on their surfaces and immersed in an electrolyte of specified hydrogen ion concentration and ionic strength. Two cylinders represent a fundamental interacting unit and to understand complex arrays we must first understand the simpler two cylinder problem. The electrostatic potential about a cylindrical polyelectrolyte is assumed to satisfy the linear Poisson-Boltzmann equation. A technique is developed to solve this equation for two interacting cylinders under the boundary condition discussed below.

As pointed out by Ninham and Parsegian (27), the D.L.V.O. theory for lyophobic colloids assumes boundary conditions at the surfaces of the particles which are not relevant to biological macromolecules. In this study the boundary condition is determined self-consistently assuming a single type of ionizable group on the surface of the polyelectrolyte. This self-consistency is based on the facts that the potential at the surface of a cylinder depends on the charge on the surface and that the charge is itself a function of the potential. This technique avoids the usual *ad hoc* assumption that the surface charge or the surface potential remains fixed as the

particles are brought together. In fact, there is a dynamic equilibrium in effect as the particles approach, with the degree of dissociation of ionizable groups at any point on the cylinder surface being a complicated function of their environment, i.e., the pH and ionic strength of the bathing medium and the degree of overlap of their double layers. The self-consistent boundary condition allows the observation of this dynamic process. Once the electrostatic potential is determined, it is used to compute the repulsive force and potential energy. Detailed calculations of the electrostatic interaction have been presented elsewhere (28), and the major features of that study are reviewed here.

The calculation of the attractive force requires the application of the Lifshitz theory to a cylindrical geometry. Direct application of the Lifshitz theory to interacting cylinders remains an unsolved problem and has not been attempted here since the detailed spectroscopic properties of the cylinders which are necessary to implement the theory are not presently available. The technique we have used is a synthesis of the old and the new methods. The *form* of the van der Waals force is calculated using a pairwise summation of individual atomic dispersion interactions. A simple application of pairwise summation is known to be at best qualitative but is expected to give a good approximation to the *form* for the interaction energy as a function of cylinder separation. In an attempt to make the formulation quantitative we have chosen a value for the Hamaker constant on the basis of calculations that have been made on simpler systems using the Lifshitz theory. The pairwise summation technique was used by Elliott (24), but by doing the integrations analytically we have avoided a twofold numerical integration he found necessary, and we have used a more recent estimate of the Hamaker constant.

ELECTROSTATIC REPULSION

This section is concerned with a review of a previous calculation of the electrostatic repulsive force and associated potential energy for the model system composed of two identical, parallel, charged cylinders immersed in an electrolyte of known pH and ionic strength (28).[1] The interaxis distance is denoted by R, the radius of the cylinders by s, and their length by L, with $L \gg s$. Fig. 1 illustrates the geometry. Each cylinder is assumed to be rigid and composed of a material of uniform density ρ and dielectric constant ϵ_i. The charge on each cylinder lies completely on its surface and is assumed to be due only to the dissociation of acidic groups with dissociation constant Z. The density of these ionizable groups is uniform and given by $\nu = 1/\mathcal{S}$, where $\mathcal{S}$ is the surface area per ionizable group. The charge due to dissociation is assumed to be spread uniformly over all equivalent portions of the cylinder, producing a surface charge density σ. The solution bathing the cylinders is specified to have a uniform dielectric constant ϵ, with $\epsilon \gg \epsilon_i$. The reservoir of this bathing solu-

[1] Reference 28 will hereafter be referred to as paper I.

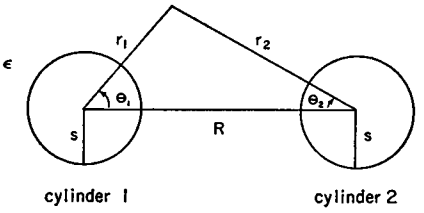

FIGURE 1 A cross-section through two parallel cylinders with two coordinate systems, one embedded in each cylinder.

tion is infinite and is of known pH and ionic strength. The entire system is at temperature T.

The quantity of primary interest in the calculation of the repulsive force is the electrostatic potential in the region surrounding the two cylinders. Once determined, this potential can be used to compute the free energy of the system. That free energy, relative to the free energy of two cylinders isolated from one another, is the work required to build the system against the electrostatic repulsive force, i.e., the interaction energy. The force follows immediately once the interaction energy is known. We require the potential, $\varphi(\mathbf{r})$, at some point outside of the cylinders to satisfy the Poisson-Boltzmann equation in its linearized form,

$$\nabla^2\varphi(\mathbf{r}) = \mathcal{K}^2\varphi(\mathbf{r}), \tag{1}$$

where $1/\mathcal{K}$ is the so-called "Debye screening length" defined by

$$\mathcal{K}^2 \equiv \frac{4\pi e^2}{\epsilon kT}\sum_j \rho_j z_j^2, \tag{2}$$

where $-e$ is the electronic charge, ϵ is the (uniform) dielectric constant of the bathing medium, T is the absolute temperature, k is Boltzmann's constant, and the sum extends over all ionic species in the reservoir with ρ_j and z_j as the number density and charge, respectively, of ions of type j. A detailed derivation of Eq. 1 in which the fundamental assumptions are clearly stated can be found in paper I.

The solution to this second-order partial differential equation requires two boundary conditions. This first condition we impose is that the potential vanish far from the cylinders because of the screening of the surface charge distributions by a diffuse layer of counterions. Secondly, the dielectric displacement is discontinuous across either cylinder boundary because of the surface charge distributions. As discussed in paper I it is appropriate to apply the constraint

$$\hat{n}\cdot\nabla\varphi(\mathbf{r}_1) = -\frac{4\pi\sigma(\theta_1)}{\epsilon} \quad \text{at} \quad \mathbf{r}_1 = (s, \theta_1), \tag{3}$$

at the surface of cylinder 1 (the cylinders are identical). We now proceed to determine $\sigma(\theta_1)$ self-consistently.

The surface charge density arises because of the dissociation of acidic groups. The charge density $\sigma(\theta_1)$ can thus be written in terms of the surface area per ionizable group $\mathcal{S}$ and the degree of dissociation $\alpha(\theta_1)$ as

$$\sigma(\theta_1) = -e\alpha(\theta_1)/\mathcal{S}. \tag{4}$$

The problem is, given $\mathcal{S}$, determine $\alpha(\theta_1)$ and thus $\sigma(\theta_1)$. The dissociation reaction is $AH \rightleftarrows A^- + H^+$, where A^- remains on the surface and H^+ moves into the bathing medium. The dissociation constant is given by

$$Z = \frac{[H^+]_{s,\theta_1}[A^-]}{[AH]} = [H^+]_{s,\theta_1}\left(\frac{\alpha}{1-\alpha}\right), \tag{5}$$

where $[H^+]_{s,\theta_1}$ is the hydrogen ion activity at the surface of the cylinder at θ_1, which is related to the hydrogen ion activity in the reservoir (which we denote by H) through the relation

$$[H^+]_{s,\theta_1} = H \exp\,[-e\varphi(s, \theta_1)/kT], \tag{6}$$

where $\varphi(s, \theta_1)$ is the surface potential on cylinder 1 at θ_1. Eq. 6 follows directly from the assumption of a Boltzmann distribution implicit in the use of the Poisson-Boltzmann equation. For consistency we must linearize Eq. 6 to obtain

$$[H^+]_{s,\theta_1} = H[1 - e\beta\varphi(s, \theta_1)], \tag{7}$$

where $\beta = (kT)^{-1}$.

It was shown in paper I that we can write a solution of Eq. 1 in the form

$$\varphi_1(r_1, \theta_1) = \sum_{n=0}^{\infty} A_n K_n(\mathcal{K}r_1) \cos\,(n\theta_1). \tag{8}$$

By symmetry, an equally good solution constructed about the second cylinder is

$$\varphi_2(r_2, \theta_2) = \sum_{n=0}^{\infty} A_n K_n(\mathcal{K}r_2) \cos\,(n\theta_2). \tag{9}$$

Following Levine (25, 26) we write the general solution as the sum of Eqs. 9 and 10

$$\varphi = \sum_{n=0}^{\infty} A_n\{K_n(\mathcal{K}r_1) \cos\,(n\theta_1) + K_n(\mathcal{K}r_2) \cos\,(n\theta_2)\} \begin{matrix} r_1 > s \\ r_2 > s \end{matrix}. \tag{10}$$

Eq. 10 is an exact solution of Eq. 1 for the two cylinder system. We now must determine the set of constants $\{A_n\}$ by applying the appropriate boundary condition, Eq. 3. We proceed as follows. Once the interaxis distance R is specified, we can

write the potential as a function of r_1 and θ_1 alone in a Fourier series,

$$\varphi = \sum_{n=0}^{\infty} f_n(r_1) \cos(n\theta_1), \qquad 0 \leq \theta_1 \leq 2\pi. \tag{11}$$

Only cosine terms are required to describe the potential because it is symmetric in θ_1. The coefficients in the Fourier decomposition are given by

$$f_n(r_1) = \left(\frac{2 - \delta_{no}}{\pi}\right) \int_0^{\pi} \varphi(r_1, \theta_1) \cos(n\theta_1)\, d\theta_1, \tag{12}$$

where δ_{no} is the Kronecker delta,

$$\delta_{nm} = \begin{cases} 1 & \text{if } n = m \\ 0 & \text{if } n \neq m. \end{cases} \tag{13}$$

Clearly, $f_0(r_1)$ is the average value of the potential at some distance r_1 from the center of cylinder 1. We also decompose $\alpha(\theta_1)$ into a Fourier series

$$\alpha(\theta_1) = \sum_{n=0}^{\infty} \alpha_n \cos(n\theta_1). \tag{14}$$

The coefficients α_n are given by

$$\alpha_n = \left(\frac{2 - \delta_{no}}{\pi}\right) \int_0^{\pi} \alpha(\theta_1) \cos(n\theta_1)\, d\theta_1, \tag{15}$$

so that α_0 is the average degree of dissociation on the cylinder surface. Substituting Eqs. 14, 11, and 4 into Eq. 3 we obtain

$$\sum_{n=0}^{\infty} \left(\frac{df_n}{dr_1}\right) \cos(n\theta_1) = \frac{4\pi e}{\epsilon \mathcal{S}} \sum_{n=0}^{\infty} \alpha_n \cos(n\theta_1) \quad \text{at} \quad r_1 = s. \tag{16}$$

Equating coefficients of the linearly independent cosine terms we obtain the set of equations,

$$\frac{df_n}{dr_1} = \frac{4\pi e \alpha_n}{\epsilon \mathcal{S}} \quad \text{at} \quad r_1 = s; \qquad n = 0, 1, 2, \ldots. \tag{17}$$

For $n = 0$ Eq. 17 provides a connection between the average surface potential and average surface charge, with higher values of n relating higher moments of the potential and charge. With Eq. 17 at our disposal we now proceed to establish self-consistency by relating the degree of dissociation to the potential via the surface hydrogen ion activity. Substituting Eq. 7 into Eq. 5 and using Eqs. 11 and 14 we obtain

$$(Z + H) \sum_{n=0}^{\infty} \alpha_n \cos(n\theta_1) - e\beta H \sum_{n=0}^{\infty} \sum_{m=0}^{\infty} \alpha_n f_m \cos(n\theta_1) \cos(m\theta_1) - Z = 0, \tag{18}$$

where the α_n are given by Eq. 17. We can write this equation in a more useful form as

$$\sum_{n=0}^{\infty} B_n \cos(n\theta_1) = 0, \tag{19}$$

where the Fourier coefficients can be determined by multiplying Eq. 18 by $\cos(l\theta_1)$ ($l = 0, 1, 2, \cdots$) and integrating. In order to satisfy Eq. 19, each B_n must be identically zero. Clearly, this is only possible when the full solution for the potential, Eq. 10, is used. In paper I it was shown that an accurate representation of the potential can be obtained by using only the $n = 0$ terms in Eqs. 10 and 19. That is, we use the approximate potential

$$\varphi^{(0)} = A_0^{(0)}[K_0(\mathcal{K}r_1) + K_0(\mathcal{K}r_2)], \tag{20}$$

with the constant $A_0^{(0)}$ determined by the equation

$$A_0^{(0)} = \frac{B - (B^2 + 4AC)^{1/2}}{2A}, \tag{21 a}$$

where the constants A, B, and C are positive and are given by

$$A = e\beta H\left\{f_0^* \left|\frac{df_0^*}{dr_1}\right| - \frac{1}{2}\sum_{n=1}^{\infty} f_n^* \frac{df_n^*}{dr_1}\right\} \quad \text{at} \quad r_1 = s,$$

$$B = (Z + H)\left|\frac{df_0^*}{dr_1}\right| \quad \text{at} \quad r_1 = s,$$

$$C = \frac{4\pi eZ}{\epsilon\mathcal{S}}, \tag{21 b}$$

where $f_n = A_0^{(0)} f_n^*$.

The solution for the potential is now complete. It was shown in paper I that given the potential we can write the free energy of our system (relative to unionized polyions) as

$$\overline{G}(R) = 2\pi sL\left[\frac{1}{\pi^2}\int_0^{\pi}\int_0^{\pi} G(R, \theta_1, \theta_2)\, d\theta_1\, d\theta_2\right], \tag{22}$$

where

$$G(R, \theta_1, \theta_2) = G_1(R, \theta_1) + G_2(R, \theta_2), \tag{23}$$

with $G_i(R, \theta_i)$ as the free energy/unit area on cylinder i at θ_i. Furthermore, $G_i(R, \theta_i)$ is given by (29)

$$\beta G_i(R, \theta_i) = -\frac{1}{2}\beta e\nu\alpha(\theta_i)\varphi(s, \theta_i) + \alpha(\theta_i)\nu \ln\frac{H}{Z}$$

$$+ \alpha(\theta_i)\nu \ln\frac{\alpha(\theta_i)}{1 - \alpha(\theta_i)} + \nu \ln[1 - \alpha(\theta_i)], \tag{24}$$

where $\alpha(\theta_i)$ and $\varphi(s, \theta_i)$ are also clearly functions of R, and ν is the density of ionizable groups on the cylinder, $\nu = 1/s$. The interaction energy at R is the amount of work necessary to bring the parallel cylinders from infinity to R (here infinity can be interpreted as a distance where the electrostatic interaction is small enough to be neglected). The average repulsive interaction energy at R is therefore given by

$$V_r(R) = \bar{G}(R) - 2G_\infty, \tag{25}$$

where $\bar{G}(R)$ is given by Eq. 22 and G_∞ is the free energy of an isolated cylinder. Clearly as $R \to \infty$, $\bar{G}(R) \to 2G_\infty$ and $V_r(R) \to 0$. The repulsive force is given by

$$F_r(R) = -\frac{dV_r}{dR}. \tag{26}$$

Substituting Eq. 26 into Eq. 25 we obtain

$$F_r(R) = -\frac{dV_r}{dR} = -\frac{d\bar{G}}{dR}, \tag{27}$$

where $\bar{G}$ is defined by Eq. 22. The term containing G_∞ does not appear in Eq. 27 because G_∞ is independent of R. It has been shown (see paper I) that the results obtained for the force as a function of R via the complete prescription above are fit extremely well by the function

$$F_r(R) = \frac{\xi e^{-\mathcal{K}R}}{\sqrt{\mathcal{K}R}}, \tag{28}$$

where ξ can be determined by a calculation of the force at a single value of R. The interaction energy is then given by

$$V_r(R) = -\int_\infty^R F_r(R)\, dR = \int_R^\infty F_r(R)\, dR. \tag{29}$$

Substituting Eq. 28 into Eq. 29 we obtain

$$V_r(R) = \xi \int_R^\infty e^{-\mathcal{K}R} \frac{dR}{\sqrt{\mathcal{K}R}}. \tag{30}$$

Let $x^2 = \mathcal{K}R$ yielding

$$V_r(R) = \frac{2\xi}{\mathcal{K}} \int_{\sqrt{\mathcal{K}R}}^\infty e^{-x^2}\, dx. \tag{31}$$

By definition, the complementary error function is given by

$$\text{erfc}\,(z) = \frac{2}{\sqrt{\pi}} \int_z^\infty e^{-t^2}\, dt, \tag{32}$$

so we find

$$V_r(R) = \frac{\pi^{1/2}\xi}{\mathcal{K}} \operatorname{erfc} \sqrt{\mathcal{K}R}. \tag{33}$$

Computation of the interaction energy using Eq. 33 gives more accurate results (because it avoids taking the difference of two similar numbers) and takes less time than the application of Eq. 25. Before presenting a summary of the results obtained for the repulsive force, we first specify the values for several parameters which characterize the interacting cylinders and the associated reservoir of bathing medium.

Table I gives the values chosen for several of the quantities of interest. The temperature of 25°C is consistent with the "room temperature" measurements made by Rome on glycerinated muscle (2, 3) and the experiments of Bernal and Fankuchen (1) on tobacco mosaic virus. The dielectric constant of the bathing medium was chosen as that of the pure solvent, water, at 25°C (30). Variations in ϵ with ionic strength are neglected, and for low salt concentrations these effects should be quite small (31).

The cylinder radius of 80 Å is in accord with the diameters of 160 and 170 Å of the myosin filaments in striated muscle and the tobacco mosaic virus particles, respectively. The surface area per ionizable group was given the value of 400 Å^2. This value is consistent with available data on the distribution of ionizable groups on cell membranes, which suggest that S for membranes lies in the range 100–800 Å^2 (ignoring the systematically overestimated values based on cell electrophoresis studies [27]). The intermediate value of 400 Å^2 was recently used by Ninham and Parsegian (27) in theoretical investigations of cell-cell interactions and with no other information available this choice of S seems reasonable.

The acidic groups on the surface of the cylinders were chosen to have a dissociation constant characteristic of carboxylic acid groups. The value of 1.5×10^{-5} mol/liter is taken as representative (27). It should be remembered that this is an "intrinsic" dissociation constant corresponding to the dissociation of an "isolated" carboxyl group (i.e., at zero ionic strength and with the absence of any electrostatic effects due to the presence of the other ionizable groups on the polyelectrolyte).

TABLE I
PARAMETERS AND CONSTANTS

Temperature	T	25°C
Boltzmann's constant	k	1.38×10^{-16} ergs/°K
Dielectric constant of bathing medium	ϵ	78.5
Cylinder radius	s	80 Å
Surface area per ionizable group	S	400 Å^2
Dissociation constant	Z	1.5×10^{-5} mol/liter ($pZ = 4.8$)

TABLE II

THE FORCE PARAMETER ξ

pH	I	ξ
	mol/liter	*dyn/cm²*
3	0.050	4.347×10^{8}
4	0.050	2.324×10^{10}
5	0.050	3.620×10^{11}
6	0.050	1.444×10^{12}
7	0.050	2.047×10^{12}
8	0.050	2.140×10^{12}
9	0.050	2.150×10^{12}
10	0.050	2.150×10^{12}
7	0.010	2.665×10^{9}
7	0.015	9.084×10^{9}
7	0.020	2.530×10^{10}
7	0.025	6.208×10^{10}
7	0.030	1.394×10^{11}
7	0.040	5.828×10^{11}
7	0.050	2.047×10^{12}
7	0.075	2.951×10^{13}
7	0.100	2.783×10^{14}

The ionic strength values associated with the tobacco mosaic virus data are quite high, ranging up to salt concentrations of 8 mol/liter. It is thus not possible to treat the virus data quantitatively within this framework. It should be noted that Bernal and Fankuchen (1) mention neither the pH at which the ionic strength measurements were made, nor the ionic strength at which the pH measurements were made, and so it is impossible to treat their data quantitatively in any case. Once the pH is specified, our model system is completely described and we can now proceed to a review of the results of the calculations. This is most simply accomplished by tabulating the values of ξ (cf. Eq. 28) as a function of the pH and ionic strength of the bathing medium. This is done in Table II (see paper I for a detailed analysis of Table II). With these values of ξ the repulsive force and interaction energy can be immediately calculated via Eqs. 28 and 33. The results for these quantities will be discussed in more detail following an analysis of the attractive force.

VAN DER WAALS ATTRACTION

Reliable techniques for the calculation of van der Waals forces between bodies of macromolecular dimensions have been developed only recently. The major strides forward in this area have come through applications of the macroscopic van der Waals theory of Lifshitz and co-workers (17, 18). For many years it was felt that direct application of the Lifshitz formalism was not feasible (32) because the de-

tailed spectroscopic data needed to implement the theory were not generally available. Ninham and Parsegian, however, have presented a simple way to incorporate a minimum of spectroscopic data into the theory and still obtain reliable results (19–23). In particular, their calculation of the attractive force between two semi-infinite water layers across a lipid film (20, 21) is in excellent agreement with the experimental value determined by Haydon and Taylor (33). By far the majority of applications of the Lifshitz theory to date are to planar geometries (19–23). Recently, Mitchell and Ninham (34) have applied the Lifshitz method to interacting spherical particles, but had to resort to difficult analysis and to numerous approximations. On the basis of their study it seems reasonable to suggest that direct application of the Lifshitz theory to nonplanar systems is by no means a trivial problem.

We must now address the problem of how to proceed with the calculation of the van der Waals force between our cylindrical polyelectrolytes. There are several important points to consider. The first is that generalization of the Lifshitz theory to cylindrical geometry in a *rigorous* way does not appear to be feasible at the present time in light of the results obtained by Mitchell and Ninham (34) for interacting spheres. The second point is that the required spectroscopic data for tobacco mosaic virus or myosin myofilaments are not readily accessible. Finally, it must be noted that in its present state of development the Lifshitz theory cannot handle the problem of the ionic double layer surrounding polyelectrolytes. It is well known that polyelectrolytes have very large polarizabilities because of the displacements of counterions and thus the van der Waals force should properly take into account the the frequency-dependent dielectric properties of the ionic atmosphere. Any calculation of the van der Waals force between polyelectrolytes which neglects this effect may therefore not be considered exact.

The above discussion argues against direct application of the Lifshitz theory to this problem. In the spirit of the old Hamaker-London theory (35, 36) we calculate the form of the attractive force by a pairwise summation of individual atomic interactions. We then use the results of the Lifshitz theory for interactions in planar lipid-water systems to "guess" a reasonable value for the so-called "Hamaker constant" which characterizes the interaction. It is important to note that the notion of a Hamaker *constant* can be quite misleading as has been shown by Ninham and Parsegian (19–23) and we use the term here advisedly. The results so obtained are expected to give quite reliable estimates for the van der Waals force between two lipid cylinders immersed in water, and the best estimates to date of the van der Waals force between polyelectrolyte lipid-like cylinders immersed in an ionic environment.

This pairwise summation technique has been the backbone of colloid stability studies for many years (16). It must be clearly stated, however, that on the basis of the Lifshitz theory calculations made by Ninham and Parsegian (19–23), this technique must be used with great care. We believe that by making a choice of the Hamaker constant on the basis of Ninham and Parsegian's studies, we can obtain a reasonably sound *estimate* of the van der Waals attraction. Pairwise summation

was used by Elliott (24), but by carrying through the summation analytically we have avoided the twofold numerical quadrature used in his study. It will also be seen that our choice of the Hamaker constant differs drastically from Elliott's. Spaarnay (37) has carried out such a pairwise summation for cylinders based on Bouwkamp's (38) calculation for flat disks. He, however, treated the Hamaker constant as an adjustable parameter.

The individual atomic interactions are represented by the form

$$v(r) = -c_6 r^{-6}, \tag{34}$$

as originally suggested by London (35) where c_6 is an interaction constant characterizing the interacting atoms and r is the distance between the atomic centers. The energy of interaction between two volume elements, say $d\mathbf{r}_1$ and $\mathbf{r}_1$ and $d\mathbf{r}_2$ at $\mathbf{r}_2$, each containing ρ atoms per unit volume, is therefore just given by $-\rho^2 c_6 |\mathbf{r}_1 - \mathbf{r}_2|^{-6} d\mathbf{r}_1 d\mathbf{r}_2$. Integrating over all $\mathbf{r}_1$ in cylinder 1 and all $\mathbf{r}_2$ in cylinder 2 we have

$$V_a(R) = -\rho^2 c_6 \int_1 \int_2 |\mathbf{r}_1 - \mathbf{r}_2|^{-6} d\mathbf{r}_1 d\mathbf{r}_2, \tag{35}$$

where R is the interaxis distance. It is convenient to build up the interaction energy as follows.

First we consider the interaction of a single atom (in cylinder 1, for example) with a row of atoms at a perpendicular distance y from this atom (in cylinder 2, parallel to the cylinder axis). The geometry is illustrated in Fig. 2 and we find for the van der Waals energy

$$v_1(y) = -\rho^{1/3} c_6 \int dz\, r^{-6} \tag{36}$$

where $\rho^{1/3}$ is the density of atoms per unit length. Now we may replace the integration over z by an integration over θ (see Fig. 2) by noting $r^2 = z^2 + y^2$ and

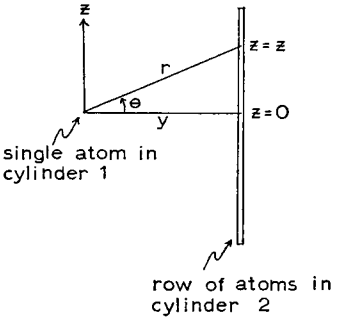

FIGURE 2 The interaction of a single atom with an infinite linear array of atoms.

$z = y(\tan\theta)$ so we find

$$v_1(y) = -\rho^{1/3} c_6 y^{-5} \int d\theta \cos^4\theta. \tag{37}$$

Because the length of the cylinders is extremely large compared with any other dimension in the system we can choose the limits of z as $\pm\ \infty$ and so the limits of θ are $\pm\ \pi/2$. The θ integration is now straightforward and thus

$$v_1(y) = -\frac{3\pi}{8} \rho^{1/3} c_6 y^{-5}. \tag{38}$$

Because we are neglecting end effects we can obtain the interaction energy for a row of atoms in cylinder 1 (containing the single atom above, and parallel to the cylinder axis) with the parallel row in cylinder 2 by simply multiplying Eq. 38 by the number of atoms in the row in cylinder 1 which is $\rho^{1/3}L$ where L is the length of the cylinder. Therefore the interaction energy between two rows of atoms of length L and a distance y apart is given by

$$v_2(y) = \rho^{1/3} L v_1(y) = -\frac{3\pi}{8} \rho^{2/3} c_6 L y^{-5}. \tag{39}$$

This result shows that the interaction between two cylinders at large separations should be proportional to R^{-5} since at large distance we have "thin" cylinders like those treated above.

We must now consider the interaction of all possible rows of atoms in the two cylinders. In Fig. 3 we have drawn a cross-section of the two cylinders indicating the distance y between two such rows. We have also drawn two cylindrical coordinate systems, one centered on the axis of each cylinder. We now consider the interaction of a row of atoms at position $\mathbf{y}_1$ in cylinder 1 with all possible rows in cylinder 2. We have, for the interaction energy

$$v_3(\mathbf{y}_1, R) = \rho^{2/3} \int d\mathbf{y}_2 v_2(y), \tag{40}$$

where $\rho^{2/3}$ is the density of atoms per unit area. Referring to Fig. 3 we see $d\mathbf{y}_2 =$

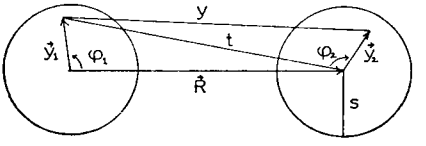

FIGURE 3 A cross-section through parallel cylinders illustrating the geometry for pairwise summation.

$y_2\, dy_2\, d\varphi_2$ with $0 \leq y_2 \leq s$ and $0 \leq \varphi_2 \leq 2\pi$ so that

$$v_3(\mathbf{y}_1, R) = -\frac{3\pi}{8}\rho^{4/3}c_6 L \int_0^{2\pi} d\varphi_2 \int_0^s dy_2\, y_2\, y^{-5}. \tag{41}$$

We write y in terms of y_2 as

$$y^2 = y_2^2 + |\mathbf{R} - \mathbf{y}_1|^2 - 2y_2 |\mathbf{R} - \mathbf{y}_1| \cos\varphi_2, \tag{42}$$

where clearly $|\mathbf{y}_2| = y_2$ and $\mathbf{R}$ is a vector drawn from the axis of cylinder 1 to the axis of cylinder 2. Let $|\mathbf{R} - \mathbf{y}_1| \equiv t$ so that

$$y^2 = y_2^2 + t^2 - 2y_2 t \cos\varphi_2. \tag{43}$$

Now we have

$$y^{-5} = t^{-5}(1 + \alpha^2 - 2\alpha \cos\varphi_2)^{-5/2}, \tag{44}$$

where $\alpha = y_2/t$ and $\alpha < 1$. We now expand the right-hand side of Eq. 44 in powers of α. The coefficients in the expansion are called Gegenbauer polynomials and are denoted by $C_n^{\nu}(\cos\varphi)$ where

$$(1 + \alpha^2 - 2\alpha \cos\varphi)^{-\nu} = \sum_{n=0}^{\infty} C_n^{\nu}(\cos\varphi)\alpha^n. \tag{45}$$

Using Eq. 45 with $\nu = 5/2$ in Eq. 44, and then substituting the result into Eq. 41 we have

$$v_3(\mathbf{y}_1, R) = -\frac{3\pi\rho^{4/3}c_6 L}{8} \int_0^s \int_0^{2\pi} dy_2\, d\varphi_2\, y_2\, t^{-5} \sum_{n=0}^{\infty} C_n^{5/2}(\cos\varphi_2)\alpha^n \tag{46}$$

Interchanging the order of summation and integration

$$v_3(\mathbf{y}_1, R) = -\frac{3\pi\rho^{4/3}c_6 L t^{-5}}{8} \sum_{n=0}^{\infty} \int_0^s dy_2\, y_2\, \alpha^n \int_0^{2\pi} d\varphi_2\, C_n^{5/2}(\cos\varphi_2); \tag{47}$$

but $\alpha = y_2/t$ so that the integration over y_2 is straightforward giving

$$v_3(\mathbf{y}_1, R) = -\frac{3\pi\rho^{4/3}c_6 L}{8t^5} \sum_{n=0}^{\infty} \left(\frac{1}{t}\right)^n \frac{s^{n+2}}{n+2} \int_0^{2\pi} d\varphi_2\, C_n^{5/2}(\cos\varphi_2). \tag{48}$$

We must now evaluate

$$I = \int_0^{2\pi} d\varphi_2 C_n^{5/2}(\cos\varphi_2) \tag{49}$$

The Gegenbauer polynomials may be written explicitly as

$$C_n^{\nu}(\cos\theta) = \sum_{p=0}^{n}\sum_{q=0}^{n}{}^{*}\frac{\Gamma\left(\frac{\nu}{2}+p\right)\Gamma\left(\frac{\nu}{2}+q\right)}{\Gamma\left(\frac{\nu}{2}\right)p!\,\Gamma\left(\frac{\nu}{2}\right)q!}\cos(p-q)\theta, \qquad (50)$$

where * on the summation indicates that the values of p and q are restricted to sum to n in each term and where $\Gamma(x)$ is the gamma function. Substituting Eq. 50 into Eq. 49 we have

$$I = 2\sum_{p=0}^{n}\sum_{q=0}^{n}{}^{*}\frac{\Gamma\left(\frac{5}{2}+p\right)\Gamma\left(\frac{5}{2}+q\right)}{\Gamma\left(\frac{5}{2}\right)p!\,\Gamma\left(\frac{5}{2}\right)q!}\int_0^{\pi}\cos(p-q)\,\varphi_2\,d\varphi_2. \qquad (51)$$

The integral over the cosine terms vanishes unless $p = q$ and so

$$I = 2\sum_{p=0}^{n}\sum_{q=0}^{n}{}^{*}\frac{\Gamma\left(\frac{5}{2}+p\right)\Gamma\left(\frac{5}{2}+q\right)}{\Gamma^2\left(\frac{5}{2}\right)p!\,q!}\pi\delta_{pq}. \qquad (52)$$

Because we are restricted to values of $p = q$ and $p + q = n$ the only term that survives in the double sum is $p = q = n/2$. Letting $n = 2m$ (since n must be even) we have

$$I = 2\pi\left[\frac{\Gamma\left(\frac{5}{2}+m\right)}{\Gamma\left(\frac{5}{2}\right)m!}\right]^2. \qquad (53)$$

Substitution of Eq. 53 into Eq. 48 yields

$$v_3(\mathbf{y}_1, R) = -\frac{3\pi^2\rho^{4/3}c_6 L}{8}\sum_{m=0}^{\infty}\frac{s^{2m+2}}{m+1}\left[\frac{\Gamma\left(\frac{5}{2}+m\right)}{\Gamma\left(\frac{5}{2}\right)m!}\right]^2\left(\frac{1}{t}\right)^{2m+5}. \qquad (54)$$

We now have the interaction energy of one row of atoms in cylinder 1 at $\mathbf{y}_1$ with all the atoms in cylinder 2. The total interaction energy can now be found by integrating over all $\mathbf{y}_1$,

$$V_a(R) = \rho^{2/3}\int_1 d\mathbf{y}_1\, v_3(\mathbf{y}_1, R). \qquad (55)$$

Referring to Fig. 2 we see that $dy_1 = y_1\, dy_1 d\varphi_1$ and $0 \leq y_1 \leq s, 0 \leq \varphi_1 \leq 2\pi$. Substituting Eq. 54 for $v_3\ (\mathbf{y}_1, R)$ into Eq. 55 we obtain

$$V_a(R) = -\frac{3\pi^2\rho^2 c_6 L}{8} \sum_{m=0}^{\infty} \frac{s^{2m+2}}{m+1} \left[\frac{\Gamma\left(\frac{5}{2}+m\right)}{\Gamma\left(\frac{5}{2}\right) m!} \right]^2 \int_0^{2\pi} \int_0^{s} d\varphi_1\, dy_1\, y_1\, t^{-(2m+5)}. \quad (56)$$

Consider the integral

$$J = \int_0^{s} \int_0^{2\pi} dy_1\, d\varphi_1\, y_1\, t^{-(2m+5)}. \quad (57)$$

We can express t as a function of R, y_1, and φ_1 by

$$t^2 = |\mathbf{R} - \mathbf{y}_1|^2 = R^2 + y_1^2 - 2Ry_1 \cos\varphi_1. \quad (58)$$

Let $\delta = y_1/R$ where $\delta < 1$. Substitute Eq. 58 into Eq. 57 and we find

$$J = \frac{1}{R^{2m+5}} \int_0^{s} \int_0^{2\pi} dy_1\, d\varphi_1\, y_1 (1 + \delta^2 - 2\delta \cos\varphi_1)^{-(m+5/2)}. \quad (59)$$

Introducing an expansion of the integrand in Gegenbauer polynomials we find

$$J = \frac{1}{R^{2m+5}} \sum_{q=0}^{\infty} \int_0^{s} \int_0^{2\pi} dy_1\, d\varphi_1\, y_1\, C_q^{m+5/2} (\cos\varphi_1)\, \delta^n. \quad (60)$$

Integrating over $y_1 (\delta = y_1/T)$ we obtain

$$J = \frac{1}{R^{2m+5}} \sum_{q=0}^{\infty} \frac{s^{q+2}}{q+2} \left(\frac{1}{R}\right)^q \int_0^{2\pi} d\varphi_1\, C_q^{m+5/2} (\cos\varphi_1). \quad (61)$$

The integral over φ_1 is of identical form with that over φ_2 in Eq. 49. Proceeding as before

$$\int_0^{2\pi} C_q^{m+5/2} (\cos\varphi_1)\, d\varphi_1 = 2\pi \left[\frac{\Gamma\left(\frac{5}{2}+m+\frac{q}{2}\right)}{\Gamma\left(\frac{5}{2}+m\right)(q/2)!} \right]^2, \quad (62)$$

with q even. Let $n = q/2$ and substitute Eq. 62 into Eq. 61 to get

$$J = \frac{1}{R^{2m+5}} \sum_{n=0}^{\infty} \frac{s^{2n+2}\pi}{(n+1)R^{2n}} \left[\frac{\Gamma\left(\frac{5}{2}+m+n\right)}{\Gamma\left(\frac{5}{2}+m\right) n!} \right]^2. \quad (63)$$

Now substitute Eq. 63 for J into Eq. 56 for the interaction energy and we obtain

$$V_a(R) = -\frac{3\pi AL}{8R\Gamma^2\left(\frac{5}{2}\right)} \sum_{m=0}^{\infty}\sum_{n=0}^{\infty} \frac{\Gamma^2\left(\frac{5}{2}+m+n\right)}{(m+1)!(n+1)!m!n!}\left(\frac{s}{R}\right)^{2n+2m+4}, \quad (64)$$

where we have introduced the Hamaker constant $A = \pi^2\rho^2 c_6$. We may rewrite this as

$$V_a(R) = -\frac{2AL}{3R} \sum_{m=1}^{\infty}\sum_{n=1}^{\infty} \frac{\Gamma^2\left(m+n+\frac{1}{2}\right)}{m!n!(m-1)!(n-1)!}\left(\frac{s}{R}\right)^{2(m+n)}, \quad (65)$$

where we have used the fact that $\Gamma(5/2) = 3/4\Gamma(1/2) = 3\pi^{1/2}/4$ and have changed the limits on the sums. Eq. 65 is the result we were after. Notice that as $R \gg s$ we find $V(R) \propto R^{-5}$ as was suggested below Eq. 39. It should be noticed that this series converges for all $R \geq 2s$, albeit rather slowly as $R \to 2s$ and the cylinders' surfaces touch.

The attractive force is given by

$$F_a(R) = -\frac{dV_a}{dR},$$

$$= -\frac{2AL}{3R^2} \sum_{m=1}^{\infty}\sum_{n=1}^{\infty} \frac{\Gamma^2\left(m+n+\frac{1}{2}\right)(2m+2n+1)}{m!n!(m-1)!(n-1)!}\left(\frac{s}{R}\right)^{2(m+n)}. \quad (66)$$

This completes our derivation of the equations for the attractive energy and force. We write the energy in reduced units as

$$V_a^*(R) = \frac{V_a(R)}{L} = -\frac{2A}{3R} \sum_{m=1}^{\infty}\sum_{n=1}^{\infty} \frac{\Gamma^2(m+n+1/2)}{m!n!(m-1)!(n-1)!}\left(\frac{s}{R}\right)^{2(m+n)}. \quad (67)$$

$V_a^*(R)$ is given in units of kT per micron of cylinder length where $kT = (1.38 \times 10^{-16}\ \text{erg°K}^{-1})\ (298°\text{K}) = 4.11 \times 10^{-14}$ erg. In order to apply Eq. 67 we must merely specify the cylinder radius s and the Hamaker constant A.

To be consistent with the electrostatic calculations presented previously we choose $s = 80$ Å. We choose the value of A to be consistent with the Lifshitz calculations of Ninham and Parsegian (19, 20) on hydrocarbon-water systems. They found $A = 5.6 - 6.1 \times 10^{-14}$ erg and we arbitrarily select $A = 5.8 \times 10^{-14}$ erg from this range as representative of the Hamaker constant for the hydrocarbon cylinder system interacting through an aqueous medium.[2] This is in contrast to the value of 10^{-12} erg used by Elliott (24) (based on an early rule-of-thumb estimate made by

[2] Gingell and Parsegian (39) have recently modified the range of A to $3.4\text{–}6.8 \times 10^{-14}$ erg.

Verwey and Overbeek [16]) which is in error by a factor of the order of 10^2 for lipid-water interactions in planar geometries.

Eq. 67 can be rewritten in the following way

$$V_a^*(R) = -\frac{1}{R^5}\sum_{i=0}^{\infty} D_i\left(\frac{s}{R}\right)^{2i}, \tag{68}$$

which explicitly illustrates the interaction energy as a power series with the leading term (which is dominant at large separations) proportional to R^{-5}. The coefficients D_i can be determined directly from Eq. 67. The $i = 0$ term includes the $m = n = 1$ terms in the double summation, the $i = 1$ term includes the $m = 1$, $n = 2$ and $m = 2$, $n = 1$ terms, etc. With the parameters given above, the coefficients D_i were calculated and the summation at each R was carried out until the addition of the next term did not change the eighth significant digit. The first few D_i are given in Table III. At $R - 2s = 100$ Å the use of just this set of nine coefficients gives the attractive energy to four significant figures. At $R - 2s = 20$ Å it requires 49 terms to give 8 significant figures in V^*, while at $R - 2s = 300$ Å it requires only 6. It should be noted that the $i = 0$ term, which corresponds to the interaction of "thin" cylinders, gives only 47% of the interaction energy at $R - 2s = 100$ Å while it gives 82% at $R - 2s = 300$ Å. This is, of course, because the cylinders appear effectively thinner as they are separated to large distances.

The results for $V_a^*(R)$ are summarized in Fig. 4, where $-V_a^*(R)$ is plotted vs. $R - 2s$. The contribution of the R^{-5} term vs. separation is illustrated as well. Notice that the scale is logarithmic so that we are seeing large changes in V_a^* with R, from about $4kT/\mu$m at $R - 2s = 40$ Å to about $4 \times 10^{-2}\, kT/\mu$m at $R - 2s =$

TABLE III

THE FIRST FEW COEFFICIENTS IN A $1/R$ EXPANSION OF THE VAN DER WAALS INTERACTION ENERGY

$$V_a^*(r) = -\frac{1}{R^5}\sum_{i=0}^{\infty} D_i\left(\frac{s}{R}\right)^{2i}$$

i	$D_i \times 10^{-11}$ (kT Å$^5/\mu$m)*
0	6.80443
1	4.25277×10^{1}
2	2.17068×10^{2}
3	1.02565×10^{3}
4	4.65388×10^{3}
5	2.05989×10^{4}
6	8.96606×10^{4}
7	3.85594×10^{5}
8	1.64333×10^{6}

* $T = 298$°K, $A = 5.8 \times 10^{-14}$ erg.

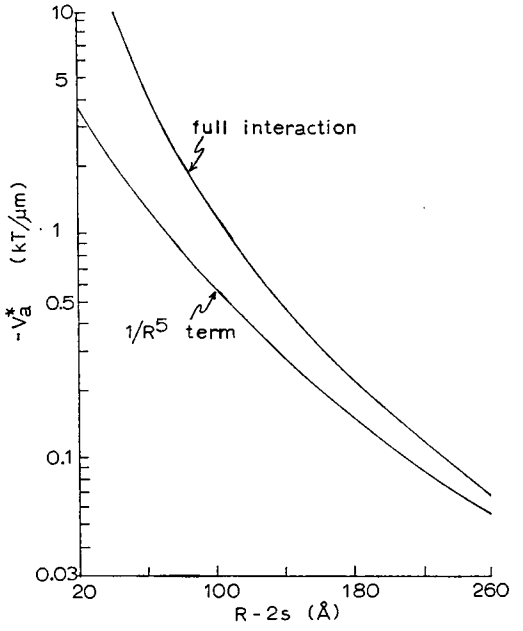

FIGURE 4 The reduced attractive potential energy. The leading $1/R^5$ term is plotted separately for comparison.

300 Å. Note also how the R^{-5} curve and full V_a^* curve converge as R increases. Because the scale is logarithmic, however, it is clear that it is not a good approximation to keep only the R^{-5} term unless R is very large.

Recently, Parsegian (40) presented an analysis of the interaction of "thin" cylinders using the Lifshitz technique and suggested that the results could have direct bearing on systems such as tobacco mosaic virus and muscle protein. On the basis of the analysis presented here it appears that the advantages gained by the applicability of the Lifshitz formulation to thin cylinders may be counterbalanced by the fact that at the interaxis separations of interest the cylinders are not, in fact, thin.

We will now combine the results found here with the repulsive electrostatic force analyzed in the last section and examine the possibility of a balance between the repulsive and attractive forces at reasonable values of the interaxis distance R.

FORCE BALANCES

The balance between the repulsive and attractive forces was examined at pH 7 as a function of the ionic strength of the bathing medium. The results are given in Figs. 5–7 and Table IV. In Fig. 5 the repulsive and attractive forces are plotted on a logarithmic scale vs. the intersurface separation (at $\theta_1 = \theta_2 = 0$) for several different ionic strength values. The general behavior can be summarized by noting that

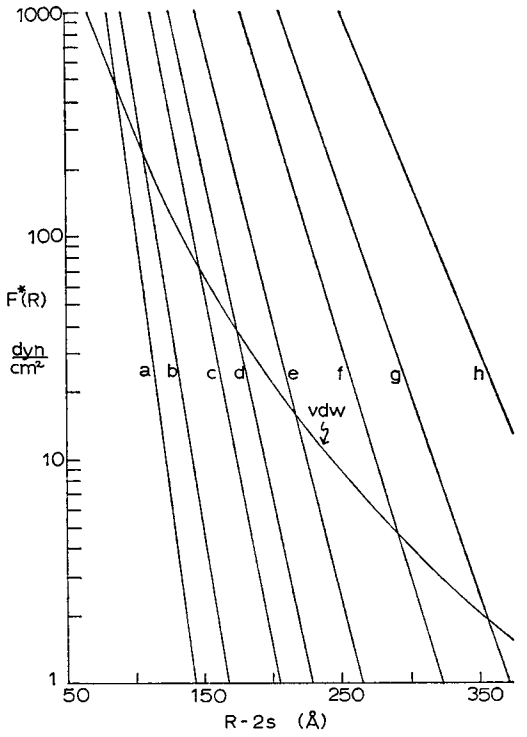

FIGURE 5 The reduced repulsive and attractive forces for several ionic strengths at pH 7. Curves a–h are repulsive forces at ionic strengths of 0.10, 0.075, 0.050, 0.040, 0.030, 0.020, 0.015,and 0.010 mol/liter, respectively. The curve vdw is the van der Waals attractive force.

whenever the repulsive force curve lies above the attractive curve the net force is repulsive, while whenever the repulsive force lies below the attractive force the net force is attractive. At that point where the repulsive and attractive force curves cross there is no net force on the cylinders. That point is the balance point.

Notice that the balance point is a strong function of ionic strength, with increasing ionic strength yielding a force balance at smaller interaxis distances. Increased ionic strength leads to decreased repulsive force because of the thinning of the double layer, i.e., the surface charge density is screened more effectively as we increase the concentration of counterions in solution. Thus the repulsive part of the potential is not felt as strongly by the cylinders as the ionic strength is increased at fixed R, and so as the ionic strength increases the balance point shifts to a smaller value of R. Notice that plots of the force allow the balance point to be located very accurately.

In Fig. 6 there is a plot of the balance point (which we will call R_m) vs. ionic strength. As discussed above R_m decreases with increasing ionic strength. The nonlinear behavior is due to the dependence of the thickness of the ionic atmosphere on the ionic strength. Projecting these results to higher values of the ionic strength we

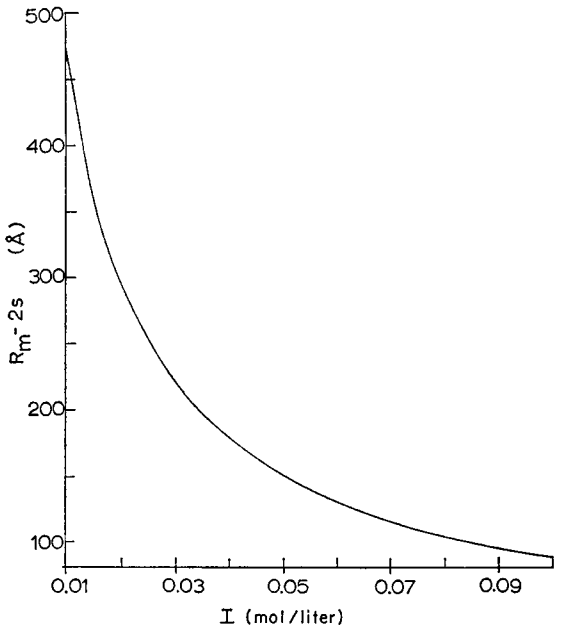

FIGURE 6 The position of the force balance as a function of ionic strength at pH 7.

expect that a value of I will be reached at which the surface charge is screened so effectively that the attractive force will be greater than the repulsive force for all separations and the most stable position will be the cylinders in contact. That is, at some value of I the value of R_m will reach a saturation value corresponding to the minimum separation possible between the cylinders.

In Fig. 7 we have plotted the total interaction energy curves vs. intersurface distance at pH 7 and for various ionic strength values. The quantity $V_t^*(R)$ is calculated from the equation

$$V_t^*(R) = V_r^*(R) + V_a^*(R), \tag{69}$$

where $V_r^*(R)$ is the reduced repulsive interaction energy defined by

$$V_r^*(R) = \frac{2\pi^{3/2} s\xi}{\mathcal{K}} \operatorname{erfc} \sqrt{\mathcal{K}R}, \tag{70}$$

where $\mathcal{K}$ is given in angstroms^{-1}, s is given in angstroms, and $\xi^* \equiv \xi \times 10^{-20}$. The units of $V_r^*(R)$ are ergs per micron of cylinder length. $V_a^*(R)$ is the reduced attractive interaction energy defined by Eq. 67. The total interaction energy (in units of kT) can be obtained by multiplying $V_t^*(R)$ by L, where L is the length of the (identical) cylinders in microns. The minimum in these interaction curves occurs at $R = R_m$ (when $R = R_m$ then $dV/dR = 0$ or $F = 0$ where F is the net force). Note

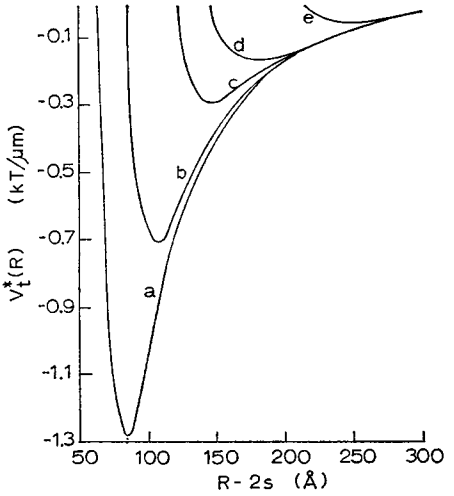

FIGURE 7 The total reduced interaction energy for several ionic strengths at pH 7. Curves a–e are for ionic strengths of 0.10, 0.075, 0.050, 0.040, and 0.025 mol/liter, respectively.

that the behavior of R_m vs. I discussed above is seen here, i.e., increased ionic strength yields decreased R_m. The new information contained in Fig. 7 is the *strength* of the interaction at R_m which is of paramount importance in discussing the stability of the system. Notice that the depth of the energy well increases with increasing ionic strength. This is because the magnitude of the attractive energy increases as R decreases more rapidly than the repulsive energy does. Since R_m decreases with increasing ionic strength, the well depth increases.

The results obtained for the behavior of the force balance as a function of ionic strength at pH 7 are summarized in Table IV. The Debye length is included for reference at each ionic strength. Note the strong effect of ionic strength on both R_m and $V_t^*(R_m)$. The general behavior seen here should be preserved at different pH values and for different choices of parameters such as the surface area per ionizable group. We conclude that at fixed pH an increase in ionic strength will lead to a decrease in the interaxis separation at which the repulsive and attractive forces are equal, and that the strength of the interaction, as measured by the depth of the potential energy well, will be larger at this decreased value of R_m.

The balance between the repulsive and attractive forces was examined at a fixed ionic strength of $I = 0.05$ mol/liter as a function of the pH of the bathing medium. The results are presented in Figs. 8–10 and Table V.

In Fig. 8 the repulsive and attractive forces are plotted on a logarithmic scale vs. the intersurface separation for several different pH values. The existence of a balance is seen at pH values greater than 4 with no crossing of the repulsive and attractive curves at pH $\leq$ 4. The general behavior that is observed is that an increase in pH corresponds to an increase in the value of R_m. The balance point is

TABLE IV

FORCE BALANCES AS A FUNCTION OF IONIC STRENGTH AT pH 7

I	$1/\mathfrak{K}$	$R_m - 2s$‡	$-V_T^*(R_m)$
mol/liter	*Å*	*Å*	*kT/μm*
0.010	30.4	474	0.006
0.015	24.8	356	0.016
0.020	21.5	290	0.034
0.025	19.2	246	0.059
0.030	17.6	214	0.092
0.040	15.2	174	0.181
0.050	13.6	147	0.299
0.075	11.1	108	0.713
0.100	9.61	86	1.290

‡ s = 80 Å.

strongly dependent on pH up to about pH 8 when further increases in pH produce no shift in the position of R_m.

We have found that increasing the pH increases the degree of dissociation of the acid groups by increasing the surface pH. The increased surface charge leads to an increased repulsion and so the repulsive force at any R increases as the pH is increased. This explains the shift in the balance point to larger R as the pH is raised. The effect of pH on the repulsive force diminishes at pH $>$ 7 because at these pH values, essentially all of the surface groups are ionized and so further increases in pH at constant ionic strength produce no significant change in the system.

In Fig. 9 we present a plot of the position of the balance point as a function of pH at I = .0.05 mol/liter. As discussed above R_m increases with pH reaching a saturation value at about pH 8 above which an increase in pH yields no change in R_m. For pH $\leq$ 4 no crossing of the force curves occurs and the attractive curve always lies above the repulsive one. There is insufficient dissociation of surface groups at these pH's to develop a significant enough repulsive force to counterbalance the attraction and the cylinders are most stable when they are at $R_m = 2s$, i.e., when they are touching.

In Fig. 10 we have plotted the total interaction energy against intersurface distance for several pH values. This provides information about the strength of the interaction. We see the minimum in the potential energy curve occurs at all pH's considered except pH 4 and no minimum is found at that pH as expected from the force results discussed above. The position of R_m increases with increasing pH as we have already seen while the depth of the well decreases with increasing pH. This is a result of the fact that the magnitude of the attractive energy increases as R decreases more rapidly than the repulsive energy does. Since R_m increases as the pH increases, the well depth must decrease.

The results obtained for the behavior of the force balance as a function of pH at

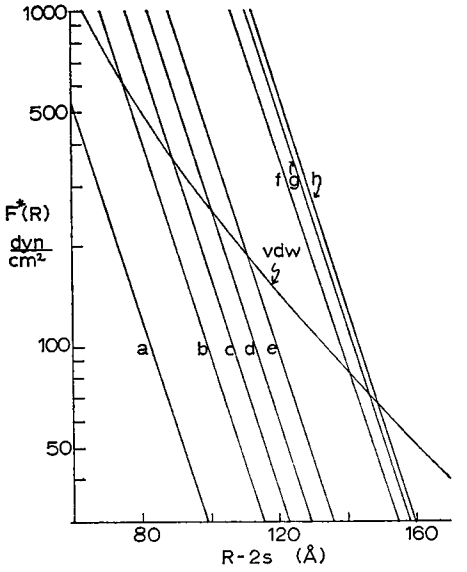

FIGURE 8 The reduced repulsive and attractive forces for several pH values at $I = 0.05$ mol/liter. Curves a–g are for pH values of 4.0, 4.4, 4.6, 4.8, 5.0, 6.0, and 7.0, respectively. Curve h is for pH values of 8, 9, and 10. The curve vdw is the van der Waals force.

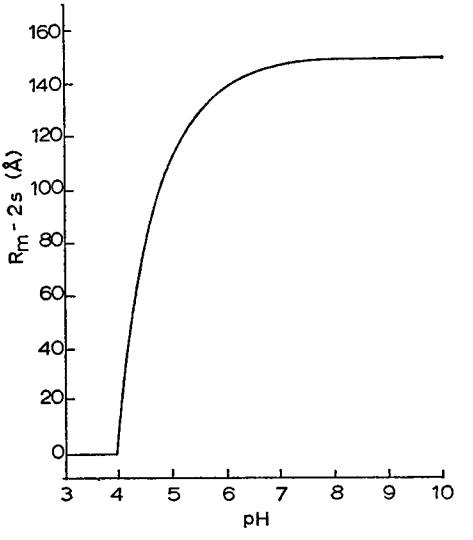

FIGURE 9 The position of the force balance as a function of pH at $I = 0.05$ mol/liter.

constant ionic strength of 0.05 mol/liter are summarized in Table V. The average degree of dissociation at each pH is included for reference. Note the strong effect of pH on both R_m and $V_t^*(R)$. We conclude that at fixed ionic strength an increase in pH will result in an increase in the interaxis separation at which the repulsive and

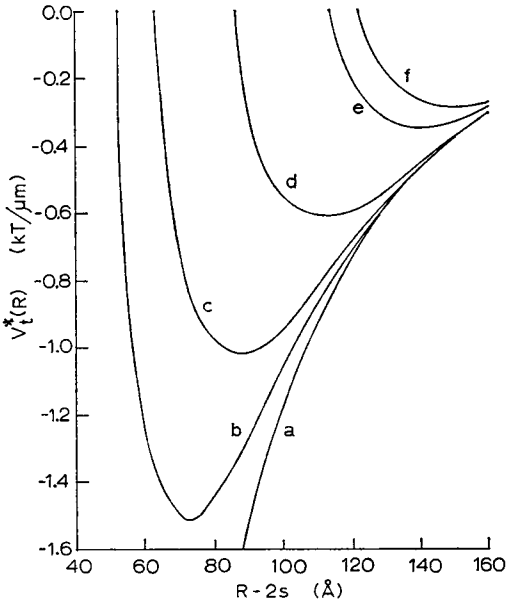

FIGURE 10 The total reduced attractive energy for several pH values at $I = 0.05$ mol/liter. Curves a–e are for pH values of 4.0, 4.4, 4.6, 5.0, and 6.0, respectively, while curve f is for pH values of 7, 8, 9, and 10.

TABLE V

FORCE BALANCES AS A FUNCTION OF pH AT $I = 0.05$ mol/liter

pH	α_0	$R_m - 2s$‡	$-V_T^*(R_m)$
	%	Å	
2.0	0.15	0	∞
3.0	1.42	0	∞
4.0	10.40	0	∞
4.2	14.45	50	2.823
4.4	19.55	71	1.509
4.6	25.72	87	1.029
4.8	32.93	100	0.775
5.0	41.03	112	0.618
6.0	81.93	140	0.342
7.0	97.56	147	0.299
8.0	99.75	148	0.294
9.0	99.97	148	0.294
10.0	99.99	148	0.294

‡ $s = 80$ Å.

attractive forces are equal, and that the strength of the interaction will be smaller at this increased value of R_m. These conclusions are expected to be valid at other values for I and for various values of the parameters which characterize the system, e.g. the cylinder radius. surface area per ionizable group, etc.

DISCUSSION

In this section we will analyze the results presented in the last section on the behavior of the balance between electrostatic repulsive forces and van der Waals attractive forces for the system of two parallel cylindrical polyelectrolytes immersed in a bathing solution as a function of the pH and ionic strength of that solution. The aim of this section is to compare our results with the experimental studies of Bernal and Fankuchen on tobacco mosaic virus (1) and the studies of Rome on the A band lattice of myosin in vertebrate striated muscle (2, 3).

The qualitative agreement between our results and those of Bernal and Fankuchen is rather striking as we shall soon see. Consider first the ionic strength results. Both systems exhibit the same behavior as salt concentration is increased. The decrease in interparticle distance as a function of increased ionic strength is well accounted for by our model. The increase of the ionic strength provides a larger amount of mobile charge which more effectively shields the surface charge on the virus, thus decreasing the repulsive force and so the interparticle distance. A saturation value is reached where no further decrease in the interparticle distance occurs as the ionic strength is raised. This occurs when the virus charge is so effectively screened that the attractive force can bring the particles into contact.

The pH data of Bernal and Fankuchen are also well explained by our colloidal model. In the region above pH 4 the interparticle distance increases with increasing pH as do our results as seen in Fig. 9. The pH curve of Bernal and Fankuchen (1) exhibits a minimum at pH 3.4. Our pH curve, Fig. 9, exhibits no such minimum. This discrepancy can be explained easily within the context of our model. The surface of the virus contains basic as well as acidic groups. In fact, pH 3.4 corresponds to the isoelectric point of the virus protein (1) i.e., that point at which the net charge on the particle is zero. Below the isoelectric point the particles have a net *positive* surface charge density, and so as the pH is decreased the net positive charge increases, leading to increased repulsion. Because we have only included acidic groups we do not see the minimum. It should be clear, however, that extension of the model to include basic sites is straightforward and should yield results in good agreement with those seen in the virus system.

We will now turn our attention to Rome's results (2, 3) for the A band myosin lattice. The ionic strength curve of Rome is remarkably similar to that for tobacco mosaic virus and to Fig. 6 for the model system considered in this study, and it suffices to say that the considerations discussed above for the virus particles appear to apply here.

The pH measurements of Rome are again remarkably similar to that seen in the tobacco mosaic virus system and in our model system, Fig. 9. The muscle pH data exhibit a minimum at pH 4.7 with the interfilament spacing increasing as the pH decreases below 4.7, the isoelectric point of myosin. Thus at this point the particles have no net charge and so they are expected to be at a distance of closest approach.

For tobacco mosaic virus the minimum separation observed at the isoelectric point corresponds to direct contact of the particles. In muscle it seems probable that the projections from the myosin filaments prevent direct contact of the particles.

In general, qualitative agreement of our model with both the tobacco mosaic virus and muscle experiments is thus observed. It is quite probable that the results of Rome's studies could be fit quantitatively using this model, but because of the number of adjustable parameters this would provide little further evidence that we have a reasonable model of the actual physical situation. What is quite pleasing is that a model in which the parameters were not chosen to "fit" the experiments still yields results in excellent qualitative agreement with those experiments.

We now examine briefly the question of stability. This question is intimately tied in with the potential energy curves, Figs. 7 and 10. In order for the two cylinder system to remain at the balance point we must have $V(R_m)$ at least on the order of kT, preferably $V(R_m) \gg kT$. For the myosin filament $L \cong 1.5$ μm and so the left-hand scale in Figs. 7 and 10 should be multiplied by 1.5 to give the interaction energy for two myosin filaments. The tobacco mosaic virus particle is about 3000 Å long and so the scales should be multiplied by 0.3 to give the interaction energy of two particles. In both cases we find $V(R_m)$ is of the order of kT but not generally large enough to suggest that pairs of cylinders in solution would be highly favored except at high ionic strengths. As a kinetic unit they would probably exist for some finite time before random thermal motion would overcome the energy barrier and they would move apart. The question of stability of pairs of cylinders is not really pertinent. We are really concerned with arrays of cylinders and in such an array the well depth is in fact deeper than that seen for two cylinders. Assuming only nearest neighbors contribute, the well depth would increase sixfold. This helps, but it is probably only a part of the answer. The complete answer should include considerations of the general phenomenon of liquid-crystalline phase transitions from isotropic to nematic ordering for long rod-shaped particles. In particular, Onsager (41) has demonstrated that a transition from isotropic to nematic ordering can take place at low concentrations of rodlike particles, such as those seen in the tobacco mosaic virus studies, taking into account *only* the repulsive electrostatic interaction. This phase transition is akin to that seen in hard-rod systems (41) where now the diameter of the rods is effectively increased by the electrostatic repulsion thereby producing the transition at lower concentrations of the rods than would be expected on the basis of their actual diameter. The origin of this hard-rod transition lies in a delicate balance between the favorable entropy of the isotropic system and the fact that the ends of the rods get in each other's way. The ordering occurs when the entropic contribution to the free energy is outweighed by the energy corresponding to interference of the ends of the rods. Once the rods are ordered the considerations discussed here provide a sensitive way of determining the actual

lattice spacing. Studies are currently underway in this laboratory to determine the effects of an attractive well on this hard-rod phase transition.

CONCLUSIONS

In this study we have considered the interaction between two parallel cylindrical polyelectrolytes in an ionic bath as a model for the behavior of several rod-shaped polyelectrolyte systems of biological interest. It is likely that the results are equally applicable to other rod-like particles which form liquid-crystalline arrays. The model was analyzed to determine if a balance between the repulsive electrostatic forces and the attractive van der Waals forces could exist at reasonable separations between the cylinders.

The repulsive electrostatic force was treated by developing a general solution to the linearized Poisson-Boltzmann equation using a self-consistent boundary condition at the cylinder surfaces. The attractive force was analyzed by performing a pairwise summation of individual interatomic interactions and then choosing a Hamaker constant on the basis of modern macroscopic van der Waals theory. Finally, the attractive and repulsive forces were combined. It was found that a balance point exists between these forces and that the behavior of the balance point as a function of the pH and ionic strength of the bathing medium closely parallels that seen experimentally. We can conclude that the model system treated here provides a good representation for force balances in systems of cylindrical polyelectrolytes.

We would like to thank Professor R. H. Ottewill for kindly pointing out reference 37 and Dr. V. Adrian Parsegian for several illuminating discussions concerning the calculation of macroscopic van der Waals forces.

Dr. Brenner was a National Defense Education Act predoctoral fellow.

Received for publication 5 September 1972.

REFERENCES

1. BERNAL, J. D., and I. FANKUCHEN. 1941. *J. Gen. Physiol.* **25**:111.
2. ROME, E. 1967. *J. Mol. Biol.* **27**:591.
3. ROME, E. 1968. *J. Mol. Biol.* **37**:331.
4. WILKINS, M. H. F., A. R. STOKES, W. E. SEEDS, and G. OSTER. 1950. *Nature (Lond.).* **166**:127.
5. GOLDACRE, R. J. 1954. *Nature (Lond.).* **174**:732.
6. RANDALL, J. T., F. BOOTH, R. E. BURGE, S. FITTON JACKSON, and F. C. KELLEY. 1955. *Symp. Soc. Exp. Biol.* **9**: 127.
7. MAURICE, D. M. 1957. *J. Physiol. (Lond.).* **136**:263.
8. GRIMSTONE, A. V. 1962. *Br. Med. Bull.* **18**:238.
9. INOUÉ, S., and H. SATO. 1967. *J. Gen. Physiol.* **50** (Pt. 2):259.
10. OSTER, G. 1957. *J. Cell Comp. Physiol.* **49**:129.
11. ELLIOTT, G. F., and E. M. ROME. 1969. *Mol. Cryst. Liquid Cryst.* **8**:215.
12. SHEAR, D. B. 1969. *Physiol. Chem. Phys.* **1**:495.
13. SHEAR, D. B. 1970. *J. Theor. Biol.* **28**:531.
14. MILLER, A., and J. WOODHEAD-GALLOWAY. 1971. *Nature (Lond.).* **229**:470.

15. DERJAGUIN, S. V., and L. LANDAU. 1941. *Acta Physicochim. U.S.S.R.* **14**:633.
16. VERWEY, E. J. W., and J. TH. G. OVERBEEK. 1948. Theory of the Stability of Lyophobic Colloids. Elsevier, Amsterdam.
17. LIFSHITZ, E. M. 1956. *Sov. Phys. JETP* **2**:73.
18. DZYALOSHINSKII, I. E., E. M. LIFSHITZ, and L. P. PITZEVSKII. 1961. *Adv. Phys.* **10**:165.
19. PARSEGIAN, V. A., and B. W. NINHAM. 1969. *Nature (Lond.).* **224**:1197.
20. NINHAM, B. W., and V. A. PARSEGIAN. 1970. *Biophys. J.* **10**:646.
21. PARSEGIAN, V. A., and B. W. NINHAM. 1970. *Biophys. J.* **10**:664.
22. NINHAM, B. W., and V. A. PARSEGIAN. 1970. *J. Chem. Phys.* **52**:4578.
23. PARSEGIAN, V. A., and B. W. NINHAM. 1971. *J. Colloid Interface Sci.* **37**:332.
24. ELLIOTT, G. F. 1968. *J. Theor. Biol.* **21**:71.
25. LEVINE, S. 1939. *Proc. R. Soc. Lond. A Math. Phys. Chem.* **170**:145.
26. LEVINE, S. 1939. *Proc. R. Soc. Lond. A Math. Phys. Chem.* **170**:165.
27. NINHAM, B. W., and V. A. PARSEGIAN. 1971. *J. Theor. Biol.* **31**:405.
28. BRENNER, S. L., and D. A. MCQUARRIE. 1973. *J. Colloid Interface Sci.* In press.
29. BRENNER, S. L., and D. A. MCQUARRIE. 1973. *J. Theor. Biol.* **39.**
30. HARNED, H. S., and B. B. OWEN. 1958. The Physical Chemistry of Electrolytic Solutions. Reinhold Publishing Corporation, New York. p. 161.
31. FOWLER, R., and E. A. GUGGENHEIM. 1939. Statistical Thermodynamics. Cambridge University Press, London. pp. 394–396.
32. OVERBEEK, J. TH. G. 1966. *Faraday Soc. Discuss.* **42**:7.
33. HAYDON, D. A., and J. TAYLOR. 1968. *Nature (Lond.).* **217**:739.
34. MITCHELL, D. J., and B. W. NINHAM. 1972. *J. Chem. Phys.* **56**:1117.
35. LONDON, F. 1930. *Z. Phys.* **63**:245.
36. HAMAKER, H. C. 1937. *Physica (The Hague).* **4**:1058.
37. SPAARNAY, M. J. 1959. *Rec. Trav. Chim. Pays-Bas Belg.* **78**:680.
38. BOUWKAMP, C. J. 1947. *Proc. K. Ned. Akad. Wet. Ser. B Phys. Sci.* **50**:485.
39. GINGELL, D., and V. A. PARSEGIAN. 1972. *J. Theor. Biol.* **36**:41.
40. PARSEGIAN, V. A. 1972. *J. Chem. Phys.* **56**:4393.
41. ONSAGER, L. 1949. *Ann. N. Y. Acad. Sci.* **51**:627.